



Published in final edited form as:

AJNR Am J Neuroradiol. 2005 May ; 26(5): 1263–1269.

Prevalence of Leukoencephalopathy in Children Treated for Acute Lymphoblastic Leukemia with High-Dose Methotrexate

Wilburn E. Reddick, John O. Glass, Kathleen J. Helton, James W. Langston, Xiaoping Xiong, Shengjie Wu, and Ching-Hon Pui

From the Division of Translational Imaging Research (W.E.R., J.O.G., K.J.H., J.W.L.) and Departments of Biostatistics (X.X., S.W.) and Hematology/Oncology (C-H.P.), St Jude Children's Research Hospital; the Departments of Radiological Sciences (K.J.H., J.W.L.) and Pediatrics (C-H.P.), University of Tennessee Health Science Center; and the Departments of Electrical and Computer Engineering and Biomedical Engineering (W.E.R.), University of Memphis, Memphis, Tennessee

Abstract

BACKGROUND AND PURPOSE—An effective treatment for acute lymphoblastic leukemia (ALL), intravenous (IV) methotrexate (MTX) has a notable toxic effect on the CNS, with leukoencephalopathy (LE) being the most common form. The purpose of this study was to use objective quantitative MR imaging to prospectively assess potential risk factors on the temporal evolution of LE in patients treated for ALL.

METHODS—We evaluated the longitudinal prevalence of LE in 45 children treated for ALL in a single institutional protocol including seven courses of IV MTX and no cranial irradiation. Differences in signal intensity on T2-weighted and fluid-attenuated inversion recovery (FLAIR) images between hyperintense regions and normal-appearing genu were used to quantitatively detect LE. Cox proportional regression was used to estimate the effect of covariates (e.g., sex, MTX dose, age at diagnosis) on the prevalence of LE. After influential factors were identified, a generalized linear model was determined to predict the probability of LE in new patients. The model was necessary to facilitate statistical testing between examinations.

RESULTS—Increasing exposure, which corresponding to more courses and higher doses of IV MTX, influenced the prevalence of LE. The prevalence of LE was significant reduced approximately 1.5 years after the completion of IV MTX.

CONCLUSION—Higher doses and more courses of IV MTX placed patients at a higher risk for LE; many of the changes resolved after the completion of therapy. The effect of these changes on neurocognitive functioning and quality of life in survivors remains to be determined.

With improved treatment outcomes in children with cancer, current emphasis is placed on the survivors' quality of life, including their neurocognitive function. Acute lymphoblastic leukemia (ALL) is the most common childhood cancer, diagnosed in 3000 children annually in the United States. The 5-year event-free survival rate for pediatric patients with ALL is approximately 80% (1). Methotrexate (MTX) given intravenously (IV) at high doses has been shown to decrease hematologic, testicular, and CNS relapses. However, it has a significant toxic effect on the CNS and can potentially lead to severe neurologic morbidity. Leukoencephalopathy (LE), seen as white matter hyperintensities on T2-weighted MR imaging, is the most common manifestation, and it may be either persistent or transient (2).

The frequency and severity of LE may depend on the dose, cumulative exposure, and other clinical variables.

Before 1990, CT examinations were used to investigate the occurrence of LE in patients with ALL who were treated with intrathecal MTX and cranial radiation therapy (CRT) (3-7). The investigators used quantitative measures of ventricular size and white matter attenuation, as well as qualitative assessment of intracranial calcifications, to determine the prevalence of LE in this patient population. The prevalence of LE ranged from 9% to 35% (median, 22%), depending on when the evaluations were performed. Although CT examinations are still used in some institutions, they are increasingly replaced with MR imaging (8-14). As in previous studies, the prevalence of LE varies according when the evaluations are performed, ranging from 0% to 9% during therapy and from 16% to 69% (median, 35%) after therapy (Table 1). The study by Chu et al (14) is not included in the reported ranges because of the small sample size of only three subjects. Traditionally, the LE prevalence increases substantially after therapy.

Efforts to avoid the adverse neurologic and neurocognitive effects of CRT have prompted the reduction or elimination of CRT and the intensification of intrathecal chemotherapy and IV MTX in contemporary protocols (5,7,8,10-18). Many of these patients were evaluated with MR imaging. Once again, the prevalence of LE varied according to the time when the evaluations were performed, with a prevalence of 0% at baseline and at the beginning of consolidation, 18-76% (median, 38%) during therapy, and 5-53% (median, 20%) after therapy (Table 2). Because of differences in diagnostic imaging as well as in systemic and intrathecal therapy, meaningful comparison of the prevalence of LE between patients treated with previous and those treated with contemporary protocols cannot be made.

In this study, we examined the longitudinal prevalence of LE in children treated for ALL in a single institutional protocol, which included seven courses of IV MTX and multiple intrathecal therapy with MTX, hydrocortisone, and cytarabine but no cranial irradiation. Because of both the limited sample size and the consistency of intrathecal therapy and steroids across all subjects, they were not considered as influential covariates in this study. Sex, MTX dose, and age at diagnosis were assessed as possible risk factors affecting the prevalence of LE. LE was detected with an objective quantitative MR imaging approach. The prevalence of LE in this study was compared and contrasted with those of previous studies. The purpose of this study was to objectively assess the influence of risk factors on the temporal evolution of LE in patients treated for ALL without CRT.

Methods

Patient Population

Consecutive patients who were at least 1 year of age who were enrolled on our institutional ALL treatment protocol between July 30, 1998, and August 30, 1999, were eligible for this study. The diagnosis of ALL was established by means of morphologic, cytochemical, immunophenotyping, and genetic studies. Patients must have received no more than 1 week of previous therapy, which must have included only glucocorticoids. Because this study was designed to assess the longitudinal prevalence of LE in otherwise normal-appearing brain, patients with other neurologic complications, such as thrombosis, were not eligible. Written informed consent was obtained from the patient or his or her parent or guardian according to institutional review board, National Cancer Institute and Office for Human Research Protection guidelines. Fifty-three patients were enrolled on the treatment protocol. However, three patients were younger than 1 year, three died during induction, one withdrew from the protocol, and one had thrombosis at presentation. The exclusion criteria resulted in 45 patients eligible

for this study: 21 male and 24 female patients aged 1.5-18.6 years (median, 5.4 years) at diagnosis (Table 3).

Treatment and Procedure Timeline

Patients were assigned to low-, standard-, and high-risk groups on the basis of comprehensive risk classification, which included blast cell immunophenotype and genotype, presenting clinical features, and early treatment responses. All patients received seven courses of IV MTX, with doses adjusted to achieve targeted systemic exposure to eliminate individual differences due to variability in clearance (19). The plasma steady-state concentration was 33 $\mu\text{mol/L}$ in low-risk patients and 65 $\mu\text{mol/L}$ in standard- or high-risk patients; average doses of MTX required to achieve these targeted concentrations were 2.5 and 5.0 g/m^2 , respectively. Patients underwent MR examinations at four points during therapy: after one course (week 6, induction), after four courses (week 7, continuation), after seven courses (week 31, continuation), and at week 120 of continuation. Week 120 of continuation therapy was the end of therapy for the female patients, but the male patients received an additional 26 weeks of continuation therapy. The timing of this last imaging examination was chosen to ensure that all patients were evaluated at approximately the same point in therapy.

MR Imaging

LE is best visualized with a T2-weighted sequence, preferably with CSF attenuation (Fig 1). The imaging protocol was designed to simultaneously yield raw images for the segmentation procedures and images necessary for the clinical evaluation of the patients. All MR examinations were performed without contrast agent by using a 1.5-T Vision whole-body unit (Siemens Medical Systems, Iselin, NJ) with a standard circular polarized volume head coil. To minimize variability, a localizer sequence was used to determine the position of the patient in the coil. All images were acquired as 3-mm-thick contiguous oblique transverse-imaging sets defined by the most inferior extent of the genu and the splenium of the corpus callosum on the midline sagittal image. T1-weighted images were acquired with a multiecho inversion-recovery imaging sequence (TR/TE/TI/NEX = 8000/20/300/1, seven echoes). Proton density- and T2-weighted images were acquired simultaneously with a dual spin-echo sequence (TR/TE1/TE2/NEX = 3500/17/102/1). Fluid-attenuated inversion recovery (FLAIR) images were acquired with a multiecho sequence (TR/TE/TI/NEX = 9000/ 119/2470/1, seven echoes).

Quantitative MR Detection of LE

Registration methods developed by Ostuni and colleagues (20) were used to register all MR imaging sets within an individual examination. A correction for radiofrequency inhomogeneities in the imaging sets was performed with a modified renormalization transformation combined with a local contrast ratio measure for in-section correction and with polynomial modeling for correction across the sections. A combined imaging set consisting of FLAIR and T1-, T2-, and proton density-weighted MR images, as well as white matter, gray matter, and CSF a priori maps from a spatially normalized atlas were analyzed with a neural network segmentation based on a Kohonen self-organizing map (21,22). The self-organizing map essentially performed a pattern recognition task based on variations in the signal intensity properties of each point on the image. After the procedure was completed, the image was segmented into multiple tissue classes, with each one represented by a particular prototypical vector or pattern of intensity variation.

To improve the differentiation between true abnormal regions and CSF contaminated regions with high FLAIR signal intensity, an in-plane gradient magnitude threshold was added to the segmentation algorithm (23). Although CSF on the FLAIR images should be attenuated by the inversion pulse and appear dark, imperfect inversion and CSF pulsation can cause CSF at the extreme edges of the ventricles to sometimes remain bright, complicating the differentiation

of true abnormal regions. After the segmentation was completed, the segmented maps were manually classified to identify the prototypical vectors associated with normal-appearing genu and diffuse white matter hyperintensities. The prototypical vector associated with the segmented region corresponding to areas of highest signal intensity on T2-weighted and FLAIR images were compared with normal-appearing genu vectors from the same patient. This enabled each patient to act as his or her own control and adjusted for known maturational changes in the relaxation properties of white matter at young ages and for acquisition variance caused by coil loading and tuning. This quantitative method was shown to be highly reproducible and to agree with radiologists' reading of LE in 81% of cases (24).

Statistical Analysis

A Cox proportional regression was performed to estimate the effect of predictors on the development of LE. The first MR examination demonstrating development of LE was considered an event, and the number of weeks since diagnosis (corresponding to time in the treatment protocol) was the measure of time to event. Normal studies were censored, and the cumulative indices were then estimated. After the influential covariates (predictors) were identified, a generalized linear model with generalized estimating equations was applied to produce a logistic regression model that could predict the probability of LE in any patient treated in a similar protocol at any of the four time points in therapy. Changes in the modeled probability of LE between points in therapy were then tested for significance ($\alpha/0.05$).

Results

The first analysis was conducted to estimate the effect of risk arm, sex, and age at diagnosis on the development of LE. The analysis indicated that risk arm ($P = .095$) and age at diagnosis ($P = .163$) were the most likely influential covariates (predictors) to be included in the next model, but the correlation between the risk arm and age at diagnosis was highly significant ($P = .012$). Sex ($P = .571$) was not an influential covariate in this analysis and therefore not included in further analyses. Figure 2 shows the cumulative indices as a function of time since diagnosis for risk arm.

The generalized linear model was developed for two covariates—risk arm and examination time—and their interaction. Figure 3 shows the observed prevalence of LE in this cohort of patients, and Figure 4 shows the results of the model. The modeled probability (p) of developing LE at different points in therapy was generated by using the estimated coefficients shown in Table 4 and Equation 1:

$$p = \frac{e^{(\alpha + \beta_1 \text{dose} + \beta_2 \text{exam} + \beta_3 \text{exam} * \text{dose})}}{1 + e^{(\alpha + \beta_1 \text{dose} + \beta_2 \text{exam} + \beta_3 \text{exam} * \text{dose})}}$$

Substitution of the estimated coefficients from Table 4 into the equation for any given patient on a particular risk arm gave the estimated probability of the child having LE at any of the four time points in therapy. The standard error of the estimates enabled us to test for significance between risk-arms and between different points in therapy. Between the beginning of IV MTX at time point 1 and the second time point after four courses, the prevalence of LE in both groups was already significantly increased. The prevalence of LE in the standard- and high-risk group continued to be significantly increased at the third time point, whereas the prevalence of LE in the low-risk group did not significantly change. Between the completion of IV MTX at time point 3 and the fourth time point, the prevalence of LE was significantly reduced in both groups. Overall, higher doses and more courses of IV MTX increased the risk of LE (Fig 4); many of the changes resolved after the completion of therapy.

Discussion

We used an objective quantitative MR imaging approach to examine the longitudinal prevalence of LE in 45 children treated for ALL in a single institutional protocol with CNS prophylaxis, including seven courses of IV MTX. Increasing exposure, which corresponded to more courses and higher doses of IV MTX, was associated with an increased prevalence of LE. In patients in the standard- and high-risk groups, who receiving twice the dose of IV MTX, the risk of LE was higher than that in those in the low-risk group. However, even the low-risk group had a 67% probability of developing LE after seven courses. In all patient groups, regardless of risk, the prevalence of LE significantly increased after four courses of IV MTX, and the prevalence in the standard- and high-risk groups increased further with an additional three courses of IV MTX. However, the prevalence of LE was reduced by almost half between the completion of IV MTX and the last time point for both patient groups. This finding suggested that LE is mostly transient and that its prevalence may continue to decrease with longer follow-up after completion of therapy. Figure 5 illustrates the transient and persistent LE seen in these patients. Although the magnitude of our results may have been specific to this treatment protocol, the transient longitudinal pattern and the effect of covariates (predictors) should apply in other studies of IV MTX to treat children with ALL.

Our prevalence of LE can be compared and contrasted with those of previous studies of patients ALL treated with intrathecal and IT-MTX prophylaxis, with the constraint that the systemic therapeutic regimens are not identical. Both Wilson et al (15) and Chu et al (14) reported no prevalence of LE at the beginning of consolidation therapy at 8 weeks after diagnosis, whereas we observed 16% prevalence. The regions of LE were subtle and diffuse, and the increased sensitivity in detection of these regions was most likely due to the objective quantitative approach. The second time point, at the beginning of continuation therapy, had an overall prevalence of 59%, which was almost identical to the 60% Wilson et al reported (15). However, Asato et al (16), Paakko et al (10) and Chu et al (14) more recently reported prevalences of 21-38%. Our prevalence of LE after all seven courses of IV MTX at week 37 of continuation was 76% overall and identical to the prevalence Mahoney et al (18) described at 1 year after diagnosis; this rate was comparable to the prevalence of 52% Wilson et al (15) reported, also at 1 year after diagnosis. No comparable studies were identified for comparison with the fourth time point. Although our results at any time point are comparable to those of previous studies, we believe we are the first to use objective quantitative MR measures to assess the longitudinal prevalence of LE.

As with any study, ours had limitations regarding the results and conclusions. One complicating factor was the difficulty in distinguishing LE from unmyelinated or partially myelinated white matter in young children. However, the likelihood that the objective quantitative MR imaging approach led to systematic misclassification of normal developmental changes as LE in young children was not likely because of the validation procedures that were conducted in comparison to radiologists' readings. Another limitation was the limited time period covered with the MR examinations. Only a few patients were imaged after the completion of therapy, and we therefore could not determine if the remaining LE continued to resolve. Last, whether the LE changes affect the neurocognitive function and quality of life in survivors is unknown.

Conclusion

The current study showed an prevalence of LE that was comparable to that of previous studies, given the constraint that therapeutic regimens were not identical. Increasing exposure, which corresponded to more courses and higher doses of IV MTX, was a risk factor for LE. Some of the LE changes were transient, as evidenced by a significant reduction in the prevalence of LE approximately 1.5 years after the completion of IV MTX therapy. Although the magnitude of

these results may be specific to our treatment protocol, the transient longitudinal pattern and the effect of covariates are likely applicable to other studies.

Acknowledgments

The authors thank Rekha Karupiah for her efforts in processing and analyzing the MR studies and Vickey Simmons for scheduling the procedures.

Supported in part by R01-CA90246 and by Cancer Center Support grant P30-CA21765 from the National Cancer Institute, by the American Cancer Society F. M. Kirby Clinical Research Professorship and by the American Lebanese Syrian Associated Charities.

References

1. Pui C-H, Relling MV, Downing JR. Mechanisms of disease acute lymphoblastic leukemia. *N Engl J Med* 2004;350:1535–1548. [PubMed: 15071128]
2. Shuper A, Stark B, Kornreich L, Cohen IJ, Avrahami G, Yaniv I. Methotrexate-related neurotoxicity in the treatment of childhood acute lymphoblastic leukemia. *Isr Med Assoc J* 2002;4:1050–1053. [PubMed: 12489505]
3. McIntosh S, Fischer DB, Rothman SG, Rosenfield N, Lobel JS, O'Brien RT. Intracranial calcifications in childhood leukemia. *J Pediatr* 1977;91:909–913. [PubMed: 925819]
4. Peylan-Ramu N, Poplack DG, Pizzo PA, Adornato BT, Di Chiro G. Abnormal CT scans of the brain in asymptomatic children with acute lymphocytic leukemia after prophylactic treatment of the central nervous system with radiation and intrathecal chemotherapy. *N Engl J Med* 1978;298:815–818. [PubMed: 273143]
5. Ochs JJ, Parvey LS, Whitaker JN, et al. Serial cranial computed-tomography scans in children with leukemia given two different forms of central nervous system therapy. *J Clin Oncol* 1983;1:793–798. [PubMed: 6199470]
6. Brouwers P, Poplack DG. Memory and learning sequelae in long-term survivors of acute lymphoblastic leukemia: association with attention deficits. *Am J Pediatr Hematol Oncol* 1990;12:174–181. [PubMed: 2116096]
7. Ochs JJ, Mulhern RK, Fairclough D, et al. Comparison of neuro-psychologic functioning and clinical indicators of neurotoxicity in long-term survivors of childhood leukemia given cranial radiation or parenteral methotrexate: a prospective study. *J Clin Oncol* 1991;9:145–151. [PubMed: 1985164]
8. Paakko E, Vainionpaa L, Lanning M, Laitinen J, Pyhtinen J. White matter changes in children treated for acute lymphoblastic leukemia. *Cancer* 1992;70:2728–2733. [PubMed: 1423204]
9. Kingma A, Mooyaart EL, Kamps WA, Nieuwenhuizen P, Wilmink JT. Magnetic resonance imaging of the brain and neuropsychological evaluation in children treated for acute lymphoblastic leukemia at a young age. *Am J Pediatr Hematol Oncol* 1993;15:231–238. [PubMed: 8498647]
10. Paakko E, Vainionpaa L, Pyhtinen J, Lanning M. Minor changes on cranial MRI during treatment in children with acute lymphoblastic leukemia. *Neuroradiology* 1996;38:264–268. [PubMed: 8741199]
11. Hertzburg H, Huk WJ, Ueberall MA, et al. CNS late effects after ALL therapy in childhood, part 1: neuroradiological findings in long-term survivors of childhood ALL—an evaluation of the interferences between morphology and neuropsychological performance. *Med Pediatr Oncol* 1997;28:387–400. [PubMed: 9143382]
12. Paakko E, Harila-Saari A, Vanionpaa L, Himanen S, Pyhtinen J, Lanning M. White matter changes on MRI during treatment in children with acute lymphoblastic leukemia: correlation with neuropsychological findings. *Med Pediatr Oncol* 2000;35:456–461. [PubMed: 11070477]
13. Kingma A, van Dommelen RI, Mooyaart EL, Wilmink JT, Deelman BG, Kamps WA. Slight cognitive impairment and magnetic resonance imaging abnormalities but normal school levels in children treated for acute lymphoblastic leukemia with chemotherapy only. *J Pediatr* 2001;139:413–420. [PubMed: 11562622]
14. Chu WCW, Chik KW, Chan YL, et al. White matter and cerebral metabolite changes in children undergoing treatment for acute lymphoblastic leukemia: longitudinal study with MR imaging and 1H MR spectroscopy. *Radiology* 2003;229:659–669. [PubMed: 14576448]

15. Wilson DA, Nitschke R, Bowman ME, Chaffin MJ, Sexauer CL, Prince JR. Transient white matter changes on MR images in children undergoing chemotherapy for acute lymphocytic leukemia: correlation with neuropsychologic deficiencies. *Radiology* 1991;180:205–209. [PubMed: 2052695]
16. Asato R, Akiyama Y, Ito M, et al. Nuclear magnetic resonance abnormalities of the cerebral white matter in children with acute lymphoblastic leukemia and malignant lymphoma during and after central nervous system prophylactic treatment with intrathecal methotrexate. *Cancer* 1992;70:1997–2004. [PubMed: 1525778]
17. Bakke SJ, Fossen A, Storm-Mathiesen I, Lie SO. Long-term cerebral effects of CNS chemotherapy in children with acute lymphoblastic leukemia. *Pediatr Hematol Oncol* 1993;10:267–270. [PubMed: 8217544]
18. Mahoney DH Jr, Shuster JJ, Nitschke R, et al. Acute neurotoxicity in children with B-precursor acute lymphoid leukemia: an association with intermediate-dose intravenous methotrexate and intrathecal triple therapy—a pediatric oncology group study. *J Clin Oncol* 1998;16:1712–1722. [PubMed: 9586883]
19. Evans WE, Relling MV, Rodman JH, Crom WR, Boyett JM, Pui CH. Conventional compared with individualized chemotherapy for childhood acute lymphoblastic leukemia. *N Engl J Med* 1998;338:499–505. [PubMed: 9468466]
20. Ostuni JL, Levin RL, Frank JA, DeCarli C. Correspondence of closest gradient voxels: a robust registration algorithm. *J Magn Reson Imaging* 1997;7:410–15. [PubMed: 9090600]
21. Reddick WE, Glass JO, Cook EN, Elkin TD, Deaton R. Automated segmentation and classification of multispectral magnetic resonance images of brain using artificial neural networks. *IEEE Trans Med Imaging* 1997;16:911–918. [PubMed: 9533591]
22. Reddick WE, Glass JO, Langston JW, Helton KJ. Quantitative MRI assessment of leukoencephalopathy. *Magn Reson Med* 2002;47:912–920. [PubMed: 11979570]
23. Glass JO, Reddick WE, Reeves C, Pui CH. Improving the segmentation of therapy-induced leukoencephalopathy in children with acute lymphoblastic leukemia using a priori information and a gradient magnitude threshold. *Magn Reson Med* 2004;52:1336–1341. [PubMed: 15562471]
24. Reddick, WE.; Glass, JO.; Pui, CH. Presented at the 11th Scientific Meeting, International Society of Magnetic Resonance in Medicine. Toronto, Ontario, Canada: Jul. 2003 Differentiating therapy-induced leukoencephalopathy from unmyelinated white matter in children treated for acute lymphoblastic leukemia (ALL).

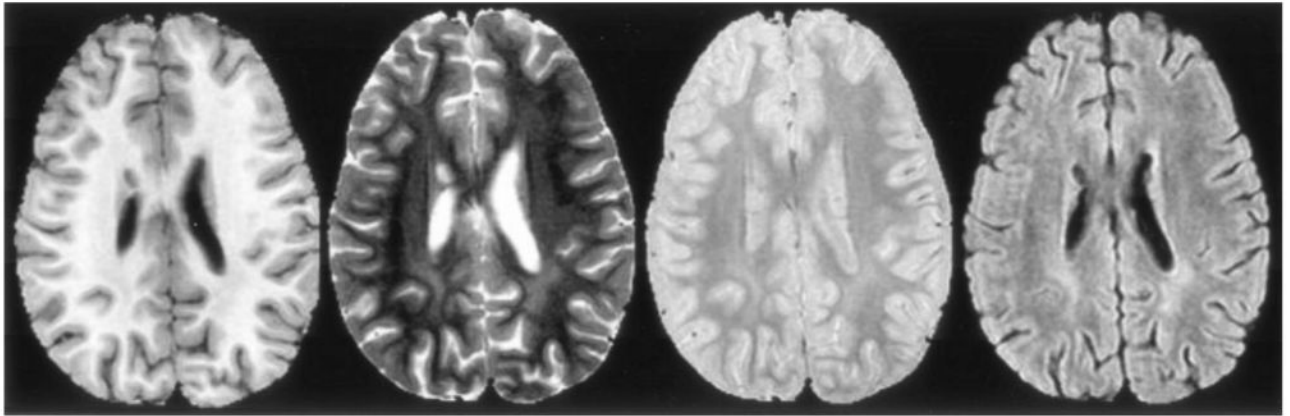


FIG 1. T1-, T2-, and proton density-weighted and FLAIR images (*left to right*) from a typical examination. LE can be seen in the white matter posterior to the ventricles.

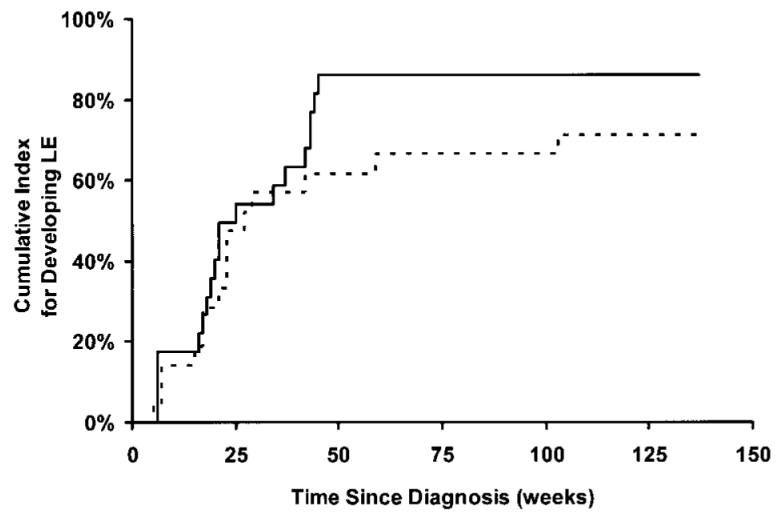


FIG 2. Cumulative risk for LE as a function of time since diagnosis. *Solid line* represents patients in the standard- and high-risk treatment arm; *dashed line*, those in the low-risk treatment arm.

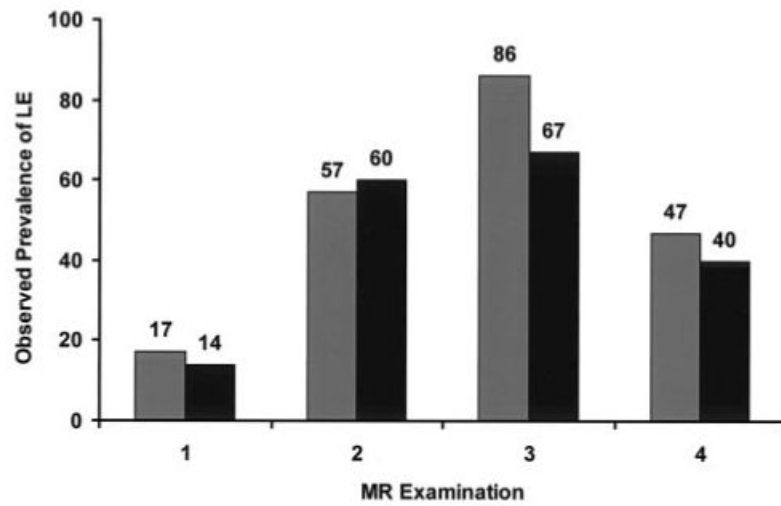


FIG 3. Observed prevalence of LE in patients in the standard- or high-risk arm (*gray bars*) and patients in the low-risk arm (*black bars*) of the treatment protocol.

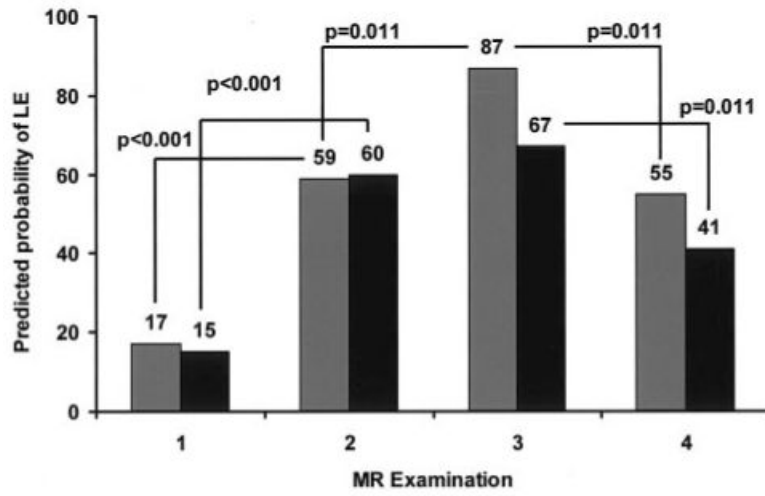


FIG 4. Predicted probability of LE according to the general linear model for patients in the standard- or high-risk arm (*gray bars*) and patients in the low-risk arm (*black bars*) of the treatment protocol.

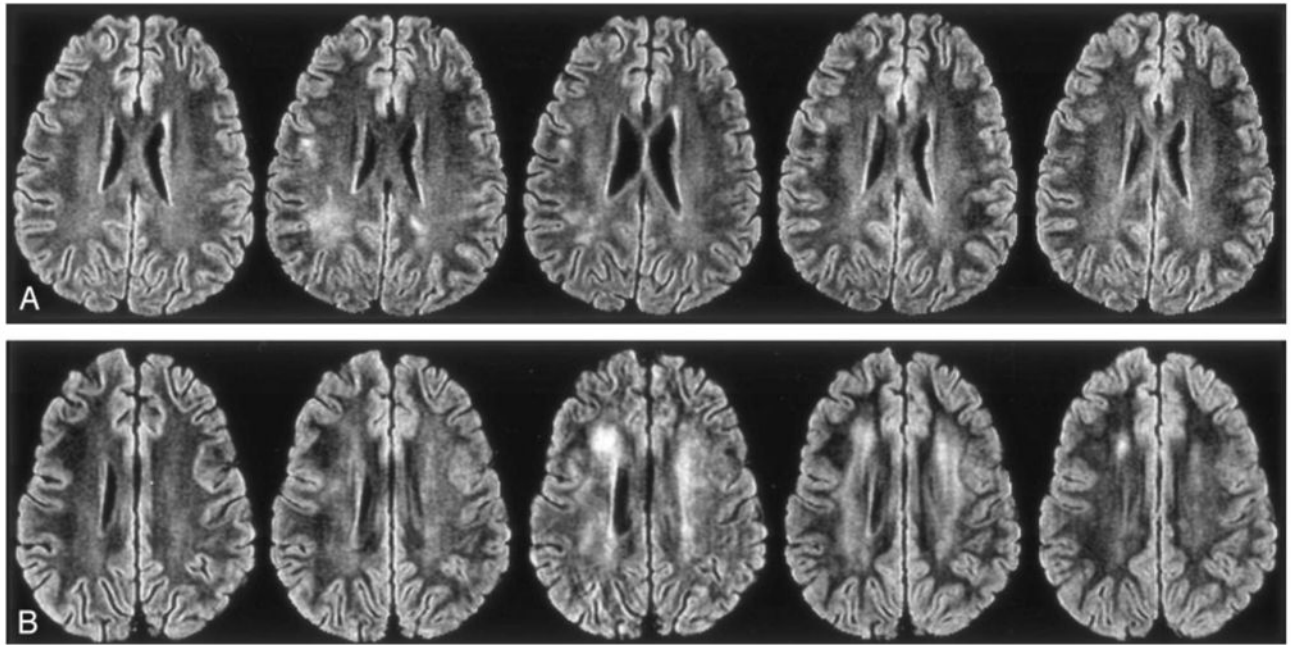


FIG 5.

FLAIR images from a typical examination. *Left to right*, Sections after one course, four courses, and seven courses of high-dose IV MTX therapy; at the end of therapy; and at 2 years after the completion of therapy.

A, Transient LE. Although the first image is normal, the second and third show LE, which resolves by the fourth and remains normal on the final image.

B, Persistent LE. First image is normal, but all others, including the 2-year follow-up image, show LE.

TABLE 1
Prevalence of LE in patients with ALL treated with intrathecal MTX and CRT prophylaxis

Study	Modality	Prevalence of LE*	Point in Therapy
Chu et al, 200314	MR imaging	0/2 (0)	Baseline
Chu et al, 200314	MR imaging	0/3 (0)	8 wk after diagnosis
Chu et al, 200314	MR imaging	1/3 (33)	20 wk after diagnosis
Paakko et al, 199610	MR imaging	0/12 (0)	End Consolidation
Ochs et al, 19835	CT	5/55 (9)	Continuation
Paakko et al, 200012	MR imaging	0/16 (0)	During
McIntosh et al, 19773	CT	10/30 (33)	0.5-6 y after induction
Peylan-Ramu et al, 19784	CT	5/32 (16)	3.5 y after diagnosis
Chu et al, 200314	MR imaging	1/3 (33)	1 year after therapy
Chu et al, 200314	MR imaging	1/2 (50)	2 y after therapy
Paakko et al, 19928	MR imaging	3/16 (19)	3 y after therapy
Chu et al, 200314	MR imaging	2/2 (100)	3 y after therapy
Brouwers and Poplack 19906	CT	5/23 (22)	4 y after therapy
Ochs et al, 19917	CT	8/23 (35)	6 y after therapy
Hertzberg et al, 199711	CT, MR imaging	23/41 (56)	6 y after therapy
Kingma et al, 19939	MR imaging	24/35 (69)	8 y after diagnosis
Hertzberg et al, 199711	CT, MR imaging	23/38 (61)	9 y after therapy
Kingma et al, 200113	MR imaging	15/24 (63)	10 y after diagnosis

* Data in parentheses are percentages.

TABLE 2
Incidence of LE in patients with ALL treated with intrathecal and IV MTX

Study	Modality	Prevalence of LE*	Point in Therapy
Wilson et al, 199115	MR imaging	0/21 (0)	Baseline
Chu et al, 200314	MR imaging	0/17 (0)	Baseline
Asato et al, 199216	MR imaging	6/16 (38)	End Induction
Chu et al, 200314	MR imaging	0/20 (0)	8 wk after diagnosis
Wilson et al, 199115	MR imaging	0/23 (0)	Beginning of consolidation
Chu et al, 200314	MR imaging	4/19 (21)	20 wk after diagnosis
Wilson et al, 199115	MR imaging	15/25 (60)	Middle of consolidation
Paakko et al, 199610	MR imaging	2/6 (33)	End of consolidation
Wilson et al, 199115	MR imaging	15/25 (60)	Begin of maintenance
Ochs et al, 19835	CT	10/53 (19)	Continuation
Paakko et al, 200012	MR imaging	3/17 (18)	During therapy
Wilson et al, 199115	MR imaging	12/23 (52)	1 year after diagnosis
Mahoney et al, 199818	CT, MR imaging	57/75 (76)	1 year after diagnosis
Chu et al, 200314	MR imaging	1/19 (5)	1 year after therapy
Chu et al, 200314	MR imaging	1/17 (6)	2 y after therapy
Paakko et al, 19928	MR imaging	1/11 (9)	3 y after therapy
Chu et al, 200314	MR imaging	2/16 (13)	3 y after therapy
Bakke et al, 199317	MR imaging	8/15 (53)	5 y after therapy
Ochs et al, 19917	CT	7/25 (28)	6 y after therapy
Hertzberg et al, 199711	CT, MR imaging	15/39 (39)	7 y after therapy
Kingma et al, 200113	MR imaging	6/16 (38)	10 y after diagnosis

* Data in parentheses are percentages.

TABLE 3
Demographic and treatment data in the 45 participants

Data	Low Risk	Standard or High Risk
No. of subjects		
After 1 course of IV MTX	21	23
After 4 courses of IV MTX	20	21
After 7 courses of IV MTX	21	21
End of Therapy	20	17
Sex		
Male	10	11
Female	12	12
Age at diagnosis (y) *	5.0 ± 2.7	9.2 ± 4.8

* Data are the mean ± standard deviation.

TABLE 4

Estimated coefficients for the general linear model to predict probability of LE during therapy

Coefficient	Estimate	Standard Error	P Value
α (intercept)	-1.77	0.625	.004
β_1 dose (g/m ²)			
5.0	0.219	0.832	.792
2.5	0.000		
β_2 exam			
First	0.000		
Second	2.181	0.632	<.001
Third	2.473	0.662	<.001
Fourth	1.423	0.548	.009
β_3 exam dose* (g/m ²)			
First and 5.0	0.000		
First and 2.5	0.000		
Second and 5.0	-0.269	0.850	.752
Second and 2.5	0.000		
Third and 5.0	0.950	1.020	.351
Third and 2.5	0.000		
Fourth and 5.0	0.338	0.793	.670
Fourth and 2.5	0.000		